Polymer 50 (2009) 1541–1547

Contents lists available at ScienceDirect

Polymer

journal homepage: www.elsevier.com/locate/polymer

Effect of side chain architecture on dielectric relaxation in polyhedral oligomeric silsesquioxane/polypropylene oxide nanocomposites

Yu Bian, Jovan Mijović*

Othmer-Jacobs Department of Chemical and Biological Engineering, Polytechnic Institute of New York University, Six Metrotech Center, Brooklyn, NY 11201, USA

ARTICLE INFO

Article history:
Received 20 October 2008
Received in revised form
5 January 2009
Accepted 10 January 2009
Available online 24 January 2009

Keywords:
Relaxation dynamics
POSS
Dielectric spectroscopy

ABSTRACT

Segmental and normal mode dynamics in polyhedral oligomeric silsesquioxane (POSS)/poly(propylene oxide) (PPO) non-reactive and reactive nanocomposites were investigated using a broadband dielectric relaxation spectroscopy (DRS) over wide ranges of frequency and temperature. Three POSS reagents with varying side chain architecture were selected for the study: OctaGlycidyldimethylsilyl (OG), TrisGlycidylEthyl (TG) and MonoGlycidylEthyl (MG). Spectra of OG and TG show a segmental (α) process at lower frequency and a local (β) relaxation at higher frequency, while MG displays only a local relaxation. Neat PPO has both segmental and normal mode (α_N) process. In POSS/PPO non-reactive nanocomposites, the presence of OG and TG causes a decrease in the time scale of α_N and α relaxation, while MG has no impact on the dynamics of PPO. Chemical reactions in POSS/PPO reactive nanocomposites lead to the formation of nanonetworks. Prior to the onset of reaction, POSS nanoparticles promote the motions of PPO chains, decrease the time scale of relaxation and give rise to thermodielectrically simple spectra. During the reaction, however, the network formation leads to spectral broadening and a gradual increase in the time scale of both segmental (α) and normal mode (α_N) relaxation. A detailed account of the effects of structure, concentration and dispersion of POSS in the matrix, molecular weight of PPO, extent of reaction and temperature on the molecular origin, temperature dependence and spectral characteristics of relaxation processes in POSS/PPO nanocomposites is provided.

1. Introduction

Inorganic–organic hybrid oligomers are of considerable interest because of their nanoscopic dimensions and the ability to enhance mechanical properties, thermal stability and oxidative resistance of polymeric matrices [1–4]. Polyhedral oligomeric silsesquioxane (POSS) is one such oligomer with a well-defined structure composed of an inorganic silica core surrounded by eight organic side groups [5–7]. Those side groups vary in architecture and can be either non-reactive or reactive with the polymer matrix. The non-reactive side groups have been shown to enhance dispersion, processing and properties of POSS/polymer nanocomposites [8–20], while the reactive side groups lead to the formation of novel copolymers [21–28] or nanonetworks [29–44].

Various side groups on the POSS cage that have been incorporated into a polymer matrix by blending or chemical tether include epoxy [45–50], amine [51], vinyl [14,26,52], styryl [21,35], methacrylate [53,54], and norbornyl [25,28,55]. While the effect of these functional groups on the macroscopic (bulk) properties of nanocomposites has been studied, missing is the information about dynamics, i.e. the time scales and the length scales of molecular motions that underlie the physical and mechanical response. Such information is important as we strive to use nanoscopic concepts to tailor macroscopic behavior.

Three POSS molecules are selected for this study; they differ in the architecture and the number of side chains attached to the POSS cage. That number is varied from one to eight. Polypropylene oxide (PPO) is used as the matrix because it contains both type A dipoles [56–59] parallel to the polymer backbone, which relax via the normal mode process, and type B dipoles perpendicular to the backbone, which relax by segmental motions. This characteristic of PPO enables us to probe the effect of architecture on dynamics at different time scales and length scales. Non-reactive and reactive end-functionalized PPO is used, each at two different molecular weights.

The objective of this study is to elucidate the effect of molecular variables that include the type, concentration and architecture of POSS nanoparticles and the molecular weight of PPO, on the dynamic features of nanocomposites. To the best of our knowledge, this study marks for the first time that Dielectric relaxation

* Corresponding author. Tel.: +1 718 260 3097; fax: +1 718 260 3125.
E-mail address: jmijovic@poly.edu (J. Mijović).

0032-3861/$ – see front matter © 2009 Elsevier Ltd. All rights reserved.
doi:10.1016/j.polymer.2009.01.036

spectroscopy (DRS) is employed to conduct an investigation of the effect of molecular architecture of POSS on the dynamics of nanocomposites.

2. Experimental section

2.1. Materials

2.1.1. Polymer

Linear polypropylene oxide (PPO) with symmetrical dipole inversion was employed in this study. Two arms emanate from a central point, each containing an uninverted dipole sequence. Each arm is end-functionalized with an amido group (*reactive*, Huntsman) or hydroxy group (*non-reactive*, Bayer). The molecular weights of PPO are 2 kg/mol (PPO2k) and 4 kg/mol (PPO4k).

2.1.2. POSS

Three POSS molecules, namely (OctaGlycidyldimethylsilyl–POSS (OG), TrisGlycidylEthyl–POSS (TG) and GlycidylEthyl–POSS (MG)), were obtained from Hybrid Plastic (www.hybridplastics.com) and used as-received. Their chemical structures are shown in Fig. 1. OG and TG are liquids at 0 °C, with a viscosity of 2.2 Pa s and 0.75 Pa s, respectively, while MG is a solid below 145 °C. The major differences between these three POSS molecules are as follows: (a) the architecture is different as shown in Fig. 1; (b) the number of functional side chains is different; OG has eight, TG has three and MG has only one; (c) the same non-reactive side chain R (R = ethyl) is present in TG and MG, but not in OG; and (d) the POSS core is a closed cage for OG and MG, and a partially open cage for TG.

2.1.3. Non-reactive nanocomposites

A desired amount of POSS was mixed with PPO with non-reactive end groups (hydroxyl groups) in toluene using a high-speed stirrer. Toluene affords good dispersion of POSS in the PPO matrix and is readily removed by evaporation. All mixtures were degassed before measurements. Identification codes for all samples studied are listed in Table 1. The first two letters stand for the type of POSS (OG, TG or MG) and the third one, "P", stands for PPO. The two numbers that follow are separated by a dash: the first one defines the molecular weight of PPO and the second one (labeled '*x*' in Table 1) indicates the weight percentage of POSS. For instance, OGP4k-10 represents the nanocomposite of POSS (OG) and PPO (P) with molecular weight of 4 kg/mol, containing 10% by the weight of OG.

2.1.4. Reactive nanocomposites

POSS was mixed with *reactive end-functionalized (amino group) PPO*, coded 'PN', in the stoichiometric ratio using the same method as for the non-reactive mixtures. The reaction is slow at room temperature. The reactive nanocomposites studied are summarized in Table 2 and a similar code was used for their identification. The percentage of POSS is not specified in the code because the mixtures are stoichiometric. For example, OGPN4k represents a reactive nanocomposite of POSS (OG) and amide functionalized PPO (PN) with molecular weight of 4 kg/mol. Note that MG/PPO nanocomposites were not prepared due to the low solubility of MG in PPO and its high concentration at the stoichiometric ratio.

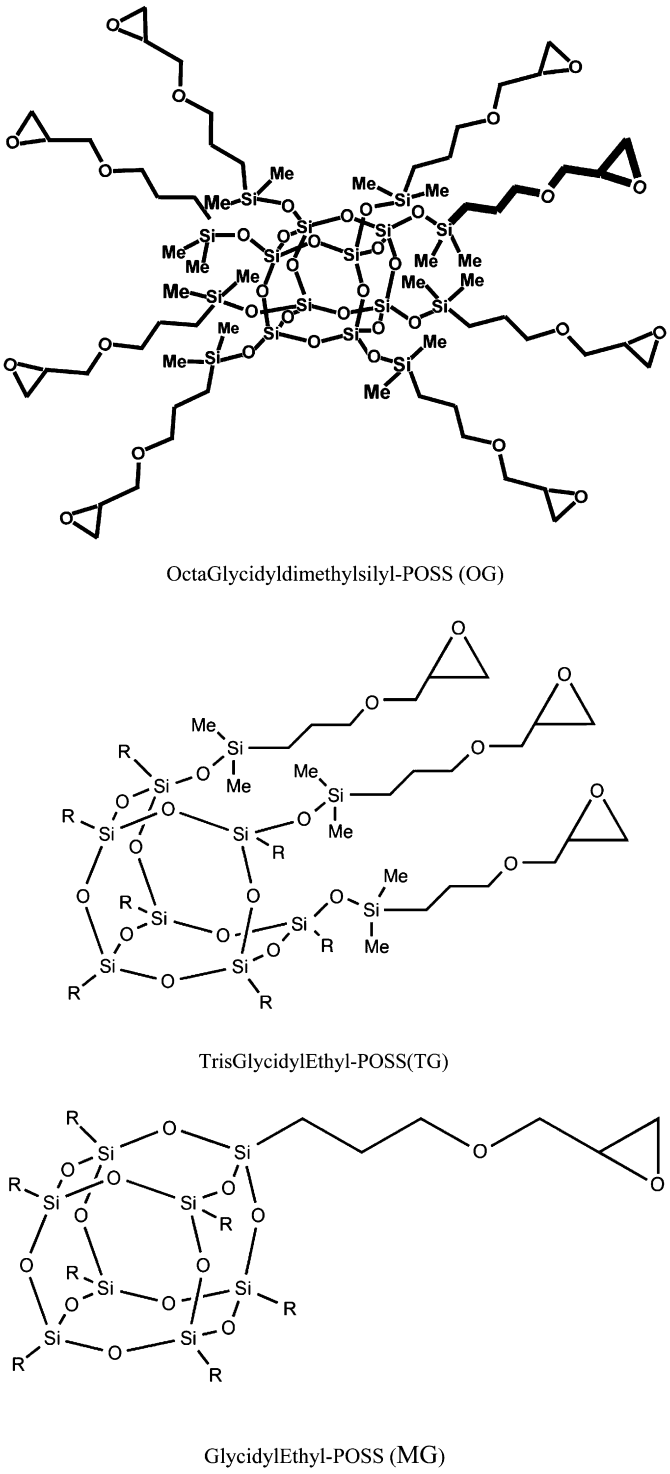

Fig. 1. Chemical structure of functionalized POSS monomers (R = ethyl).

2.2. Techniques

2.2.1. Dielectric relaxation spectroscopy (DRS)

Our facility combines commercial and custom-made instruments that include: (1) Novocontrol α high-resolution dielectric analyzer (3 μHz to 10 MHz) and (2) Hewlett–Packard 4291B RF impedance analyzer (1 MHz to 1.8 GHz). The frequency range available is from 3μHz to 1.8 GHz. The heating/cooling unit controls the sample temperature within ±0.5 °C and the experimental data are acquired through the computer connected to the instrument. In a typical DRS test, the sample is placed between the stainless steel electrodes, 12 mm in diameter and 0.05 mm in thickness and an isothermal frequency sweep conducted. Further details of our DRS facility are given elsewhere [61,62].

Table 1
OG/PPO, TG/PPO and MG/PPO non-reactive nanocomposite formulations investigated. (*x* represents the weight percentage of POSS in the system).

Description	Code
OG + PPO2k	OGP2k-x
OG + PPO4k	OGP4k-x
TG + PPO2k	TGP2k-x
TG + PPO4k	TGP4k-x
MG + PPO2k	MGP2k-x
MG + PPO4k	MGP4k-x

2.2.2. Fourier transform infrared spectroscopy (FTIR)

The FTIR spectra were obtained using a Nicolet Magna-IR 750 spectrometer with a wavenumber range from 15,800 to 50 cm^{-1} and the Vectra interferometer with a resolution smaller than 0.1 cm^{-1}. For near-infrared (NIR) measurements, the combination of a calcium fluoride beam splitter, a white light source and a Mercury–Cadmium–Tellurium (MCT) detector were used to optimize the spectra. Chemical reaction was monitored in-situ by a fiber optic sensor. The extent of reaction is obtained from the ratio of the area under the reactive (epoxy, amine) group peak at a given reaction time to the initial peak area. The results were normalized with respect to a group not involved in the reaction. The details of this technique can be found elsewhere [49].

2.2.3. Differential scanning calorimetry (DSC)

A TA Instrument Co. DSC model 2920 was employed to obtain the glass transition temperature. The heating or cooling rate was controlled at 10 °C/min.

3. Results and discussion

This section is divided into thee parts. In the first part we describe the dynamics of the individual components, POSS and PPO. In the second part we discuss the dynamics of non-reactive POSS/PPO nanocomposites. And in the third part we present the results for nanonetworks formed by the chemical cross-linking of epoxy-functionalized POSS and amine-functionalized PPO.

3.1. Individual components

The dielectric spectrum of OG in the frequency domain was described in our recent communication [45]. Briefly, OG shows two processes in the frequency range between 10^{-2} and 10^{8} Hz and in the temperature range from −100 °C to −40 °C. Both processes originate in the side chain with the functional end group and have a different time scale. The slower relaxation (lower frequency) exhibits the characteristics of the segmental (α) process in glass formers, while the faster (β) process (higher frequency) is due to the localized motions.

Dielectric loss of TG in the frequency domain (10^{-1} to 10^{8} Hz) with temperature (−100 to −20 °C) as a variable is shown in Fig. 2. The two processes observed (α and β) are similar to those in OG. But the dielectric loss of MG in the frequency domain shows only the β process in the temperature range from −100 to −70 °C (Fig. 2 inset). This process moves out of our frequency window above −70 °C. The absence of the α process in MG is the consequence of its crystalline structure. The spectral features in the low frequency region are insufficiently convincing to claim a relaxation process. It is also worth noting that the dielectric strength of the α and the β process in TG is lower than in OG at the same temperature, which is attributed to fewer functional side chains in TG. MG shows the lowest dielectric strength of the β process, because it has only one functional side chain.

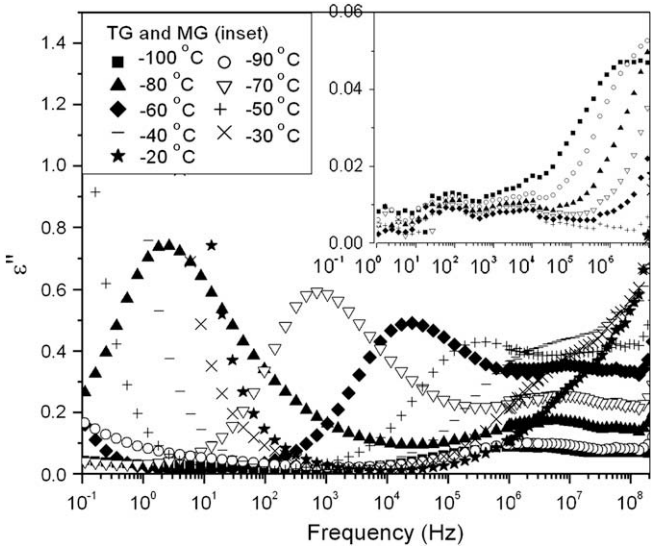

Fig. 2. Dielectric loss of TG and MG (inset) in the frequency domain with temperature as a parameter.

The temperature dependence of the average relaxation time (obtained using the Havriliak–Negami (HN) fits [67]) for each process is plotted in Fig. 3. The time scale of the α process is shorter in TG than OG, while the time scale of the β process is practically the same in all three POSS molecules. The principal dynamic characteristics of the POSS molecules studied herein can be summarized as follows: (1) segmental relaxation is faster in TG than OG due to the lower glass transition temperature ($T_g = -84$ °C for TG and −78 °C for OG); (2) the α process is not detected in MG because of its crystalline structure; (3) the temperature dependence of the β process and the activation energy (ca. 29 kJ/mol) are the same in all three POSS molecules because of the common molecular origin

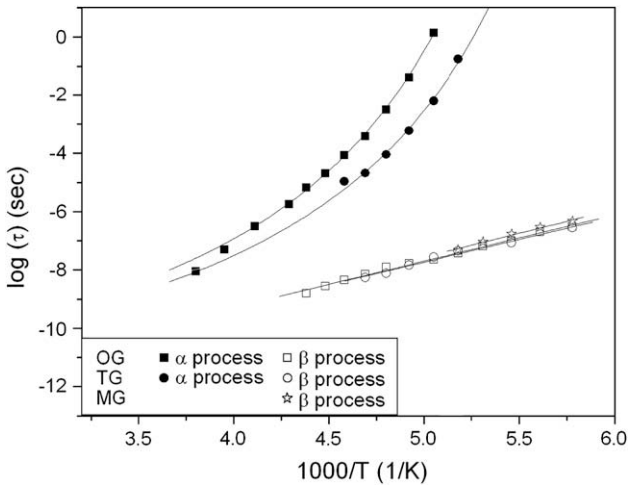

Fig. 3. Temperature dependence of the average relaxation time for OG, TG, and MG.

Table 2
OG/PPO and TG/PPO reactive nanocomposite formulations investigated.

Description	wt% of POSS in PPO matrix	Code
OG + PPO2k	31.3	OGPN2k
OG + PPO4k	18.5	OGPN4k
TG + PPO2k	42.6	TGPN2k
TG + PPO4k	27.1	TGPN4k

(the same side chain end group); (4) the lower dielectric strength of TG and MG is due to fewer functional side groups.

The dielectric relaxation of the neat PPO has been well established in the past [56–61,66], and hence we shall not be comprehensive here. Suffice it to say that the temperature dependence of the relaxation time for the segmental (τ_S) and the normal (τ_N) mode process in the neat PPO is of the Vogel–Fulcher–Tammann (VFT) type [63–65] and that an increase in the molecular weight affects the normal mode process but not the segmental process.

3.2. Non-reactive POSS/PPO nanocomposites

As reported previously [45], OGP nanocomposites display the segmental and the normal mode process observed in the neat PPO with only a slight modification in the time scale. With an increase in OG concentration, both processes shift to higher frequency (faster relaxation) and the dielectric relaxation strength ($\Delta\varepsilon_s$) of the segmental process increases. For TGP nanocomposites, the segmental and the normal mode process also shift to higher frequency with increasing TG concentration; however, $\Delta\varepsilon_s$ decreases. For MGP nanocomposites, segmental and normal mode relaxations do not shift with increasing MG concentration, but $\Delta\varepsilon_s$ decreases. The temperature dependence of the average relaxation time for both segmental and normal mode process is of the Vogel–Fucher–Tammann (VFT) type [63,64,68] in all POSS/PPO nanocomposites.

In our previous paper [45], we compared the "measured" and the "calculated" relaxation time for OGP nanocomposites in an attempt to clarify the origin of the shift in the segmental and normal mode process. The "measured" relaxation time was obtained directly from the DRS spectrum while the "calculated" value was determined from the rule of mixture using the values from the dielectric spectra of the individual components, POSS and PPO. For the segmental process, the calculated spectrum for OGP shifts to higher frequency with respect to the neat PPO due to the partial overlap with the α process in OG. Interestingly, the experimentally measured spectrum shifts to still higher frequency when compared with the calculated spectrum. This suggests that the shift of the segmental process in OGP nanocomposites is due to the combined effect of the interactions between OG and PPO and the overlap between their segmental processes. For the normal mode process, the calculated spectra of OGP do not shift with respect to the neat PPO4k but the measured spectra do, so the shift in the normal mode process in OGP is only affected by the POSS–PPO interactions. It is concluded that OG nanoparticles in the PPO matrix act as hard sphere diluents by decreasing the self-association interactions and promoting the motions of polymer chains.

We apply the same rationale to analyze the change in the dynamics of TGP and MGP nanocomposites. For TGP nanocomposites, the calculated segmental and normal relaxation times (at a given concentration) are in the same frequency range as the corresponding processes in the neat PPO, but the measured values shift to higher frequency. The segmental process of TG is faster than that of PPO (by more than one decade) and its dielectric strength is smaller than that of PPO. Thus the experimentally observed shift is interpreted as due solely to the interactions between TG and PPO. We note that the OG dynamics are characterized by a faster time scale of the segmental process and a higher dielectric strength than PPO, and that gives rise to an overlapping segmental process in OGP nanocomposites. Since TG has lower viscosity than OG, owing to fewer functional side chains and a partially open cage structure, TG nanoparticles are also a more efficient diluent in speeding up the polymer chain motions. For MGP nanocomposites, the measured and the calculated segmental or normal mode relaxation times are identical because MGP is insoluble in PPO and does not affect the chain motions. The properties of MGP nanocomposites obey the rule of mixture and hence only OGP and TGP nanocomposites are analyzed and compared below.

The average relaxation time for the segmental process in OGP2k, OGP4k, TGP2k and TGP4k nanocomposites is shown as a function of POSS concentration at −60 °C in Fig. 4. To further explore the effects of OG and TG on the dynamics of nanocomposites, we defined $\Delta\tau_S$ as the difference between the segmental relaxation time in the nanocomposite and the corresponding neat PPO at the same temperature. The principal results for $\Delta\tau_S$ are summarized as follows: (1) $\Delta\tau_S$ increases with increasing POSS concentration at any given temperature in OGP and TGP nanocomposites; (2) $\Delta\tau_S$ is greater in TGP than OGP nanocomposites for the same molecular weight of PPO; (3) $\Delta\tau_S$ increases slower in the higher molecular weight matrix. This is true for all nanocomposites and is attributed to the increased tendency of nanoparticles to form aggregates in the higher molecular weight matrix; (4) $\Delta\tau_S$ decreases with increasing temperature (not shown here) implying that POSS exerts a more pronounced effect on the dynamics of nanocomposites at lower temperature. The average relaxation time for the normal mode process in OGP and TGP nanocomposites follows a similar trend with the type and concentration of POSS, the molecular weight of PPO and temperature.

The HN parameters ***a*** and ***b*** define the spectral breadth and symmetry, respectively. For the segmental process, parameter ***b*** does not change with OG or TG concentration. Parameter ***a*** decreases (from 0.95 to 0.8) with increasing concentration in OGP but remains constant in TGP nanocomposites. For the normal mode process, the results were optimized by setting parameter ***b*** to 1, which reduces the HN equation to the Cole–Cole (CC) equation [69]. Parameter ***a*** does not change with POSS concentration in either OGP or TGP nanocomposites. Normalized loss spectra show that the segmental and the normal mode process remain thermodielectrically simple over a wide range of temperature.

The dielectric relaxation strength ($\Delta\varepsilon$), defined as $\Delta\varepsilon = \varepsilon'_0 - \varepsilon'_\infty$, where ε'_0 and ε'_∞ represent the minimum and maximum dielectric permittivity, respectively, is determined by the chemical structure and molecular architecture and as such is an important materials characteristic. $\Delta\varepsilon_S$ of OGP nanocomposites was reported to increase

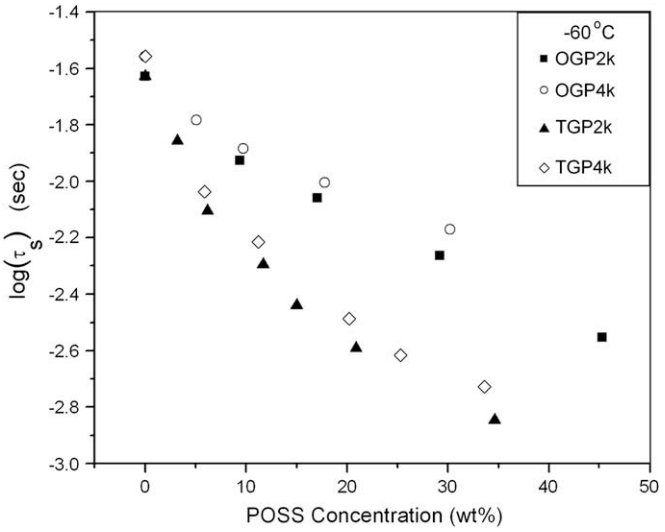

Fig. 4. Average relaxation time for the segmental process in OGP2k, OGP4k, TGP2k and TGP2k nanocomposites as a function of POSS concentration at −60 °C.

with POSS concentration [45]. This finding was attributed to the fact that the segmental process in the nanocomposites encompasses segmental processes in both PPO and OG. $\Delta\varepsilon_S$ for TGP nanocomposites decreases with increasing POSS concentration, since $\Delta\varepsilon_S$ arises from the segmental process of PPO (as described earlier). The dielectric relaxation strength of the normal mode process ($\Delta\varepsilon_N$) is a very weak (decreasing) linear function of POSS concentration in all nanocomposites.

We conclude that the effect of POSS nanoparticles on the PPO motions is determined by the surface architecture of POSS molecules. We envision POSS nanoparticle as a hard core sphere (silica cage) covered by a soft outer layer (organic side chain). POSS nanoparticles dispersed in the PPO matrix break up the self-association interactions between PPO molecules and thus exert a promoting effect on chain mobility. At the same time, however, the opposite effects are created by the newly formed interactions between PPO and the compatible functional side chains (glycidylethyl) on POSS molecules. The ensuing interplay between these two phenomena will eventually determine the time scale of the relaxation process. Our experimental results suggest that POSS with three functional side groups (TG) is most efficient in speeding up polymer motions in nanocomposites.

3.3. Reactive POSS/PPO nanocomposites

Dielectric properties of POSS/PPO nanocomposites change as POSS reacts with PPO to form nanonetworks. In this study, the chemical changes during isothermal heating of the reactive mixture were monitored with near-infrared (NIR) spectroscopy and the rate of disappearance of epoxy ($\sim$4500 cm^{-1}) and amine ($\sim$4940 cm^{-1}) groups were used to calculate the kinetics [70]. OGPN and TGPN were cured at 120° C and the extent of reaction as a function of reaction time is plotted in Fig. 5. As shown in Fig. 5, the molecular architecture of POSS and the molecular weight of PPO have an effect on the kinetics. OGPN forms faster than TGPN due to the higher concentration of reactive functional groups. The kinetics of OGPN2k (or TGPN2k) are faster than those of OGPN4k (or TGPN4k) due to the higher weight percentage of POSS in the lower molecular weight matrix.

Dielectric loss and real permittivity (inset) of TGPN2k in the frequency domain as a function of extent of reaction at −50° C are plotted in Fig. 6. Note how both segmental and normal mode process shift to lower frequency with increasing extent of reaction and the relaxation strength ($\Delta\varepsilon_s$) of the segmental process decreases. Analogous phenomena were observed for OGPN [70].

The incorporation of POSS in the PPO matrix can have both hindering and promoting effect on the dynamics of nanonetworks. On the one hand, covalent bonds that form during cross-linking hinder the motion of PPO chains. On the other hand, POSS nanoparticles act as hard sphere diluents in the polymer matrix, as seen in the non-reactive nanocomposites, and that promotes the motions of polymer chains. During the nanonetwork formation, polymer chain motions are affected by the interplay between those two phenomena. Ultimately, in the fully cured nanonetworks the promoting effect is negligible. It is also clear that τ_S and τ_N in the fully cured OGPN2k (TGPN2k) nanocomposites are longer than those in OGPN4k (TGPN4k) due to the more rigid network formed with the lower molecular weight PPO. Fully cured OGPN nanocomposites have longer τ_S and τ_N than TGPN with the same PPO molecular weight as the result of a more dense network contributed by the greater number of functional side groups in OG.

Fits of the loss spectra reveal a steady decrease in the HN parameter ***a*** during the network formation, which is the signature of spectral broadening. We define Δa as the difference in parameter ***a*** between the initial mixture and the fully cured nanonetwork. The subscripts S and N represent the segmental and the normal process, respectively. By examining Δa, we aim to clarify the effect of POSS architecture and PPO molecular weight on the spectral shape. For example: Δa_S and Δa_N at −40° C are 0.10 and 0.41 for OGPN2k, 0.05 and 0.38 for OGPN4k, 0.22 and 0.45 for TGPN2k and 0.19 and 0.40 for TGPN4k respectively. It is clear that TGPN nanonetworks have larger Δa than OGPN nanonetworks with the same PPO molecular weight due to the higher concentration of nanoparticles in the former system. In addition, nanonetworks with PPO2k have greater Δa than those with PPO4k because of the more rigid network formed with shorter PPO chains. The HN parameter ***b*** does not change with the extent of reaction for either segmental or normal mode processes at a given temperature. It is also found that the segmental and normal mode spectra become thermodielectrically complex (the unreacted mixtures are simple) following the onset of reaction. For the segmental process, parameters ***a*** and ***b*** increase

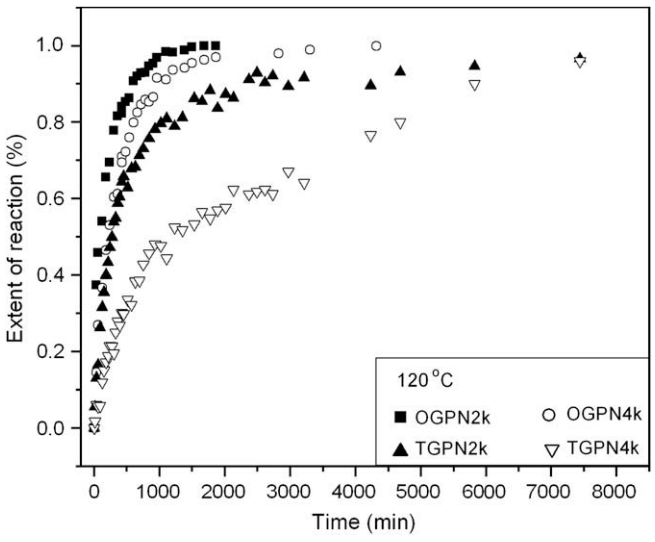

Fig. 5. Extent of reaction of OGPN2k, OGPN4k, TGPN2k and TGPN4k nanocomposites as a function of time.

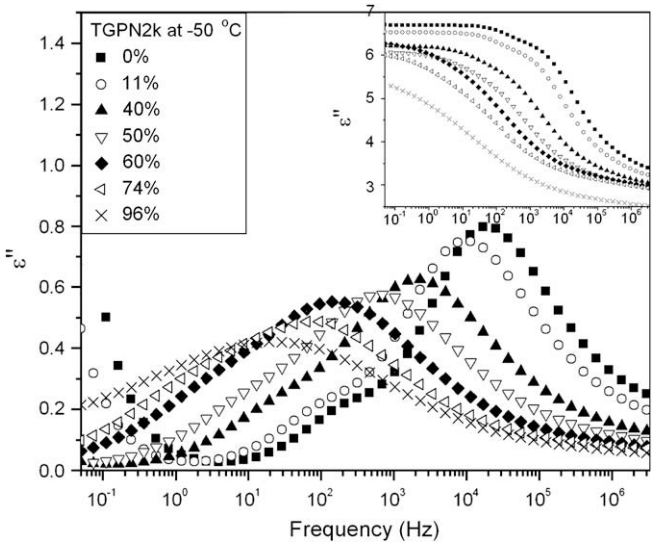

Fig. 6. Dielectric loss and permittivity (inset) for TGPN2k at −50 °C. in the frequency domain with extent of reaction as a parameter.

with increasing temperature, while for the normal mode process ***a*** increases while ***b*** remains constant at 1.

Finally, it is observed that $\Delta\varepsilon_S$ decreases with the extent of reaction, presumably because the dipolar motions are hindered by the network formation. For example, $\Delta\varepsilon_S$ of the fully cured nanonetworks decreases about 68% in OGPN2k, 37% in OGPN4k, 56% in TGPN2k and 35% in TGPN4k at -50° C. For the normal mode process, we note a monotonical increase in $\Delta\varepsilon_N$. For fully cured nanonetworks at -50° C, $\Delta\varepsilon_N$ increases about 250% in OGPN2k, 175% in OGPN4k, 340% in TGPN2k and 290% in TGPN4k. These results are consistent with the previously reported data for OC/PPO nanocomposites [70] and DGEBA/PPO composites [61], however, the underlying physics remains incompletely understood and further research is warranted.

4. Conclusions

We have completed an investigation of the dynamics of non-reactive and reactive POSS/PPO nanocomposites using broadband dielectric relaxation spectroscopy. The effect of concentration and architecture of POSS and molecular weight of PPO on dynamics was evaluated and the following conclusions were drawn.

Three POSS molecules (OG, TG and MG) were selected for this study, with varying number (one to eight) and architecture of the functional side chains. Both segmental and local relaxations were observed in OG and TG, while only the local process was seen in MG due to its crystalline structure. The time scale of the segmental process in OG is longer than that in TG due to its higher glass transition temperature. The local process has the same molecular origin in all POSS molecules and hence the same relaxation characteristics and activation energy.

In non-reactive POSS/PPO nanocomposites, the nanoparticles dispersed in the PPO matrix act as hard sphere diluents and thus promote the motion of polymer chains. The time scale of the segmental and the normal mode process decreases with increasing POSS concentration in OGP and TGP nanocomposites, but does not vary in MGP nanocomposites due to the low solubility of MG in the PPO matrix. The promoting effect of POSS is determined by its surface architecture. Of the three POSS molecules investigated TG is the most efficient in decreasing the time scale of segmental relaxation in nanocomposites. The molecular weight of PPO has an effect on dynamics. At a given POSS concentration, segmental and normal mode relaxations shift to higher frequency in the lower molecular weight matrix due to the better dispersion of nanoparticles.

In POSS/PPO nanonetworks, the covalent bonds between POSS and PPO hinder molecular motions and slow down relaxation processes. The promoting effect of POSS is noted prior to the onset of reactions but it weakens progressively compared to the hindering effect due to cross-linking. The segmental and the normal mode process in nanonetworks become slower and broader in the course of the reaction. The properties of the fully cured POSS/PPO nanocomposites are controlled by the network architecture. Slower segmental and normal mode relaxation in OGP than TGP nanonetworks is the consequence of higher cross-link density in the former imparted by eight functional side groups on OG. Also, slower segmental and normal mode relaxation and broader spectra are observed in fully cured OGP2k (or TGP2k) compared with OGP4k (or TGP4k), because PPO with lower molecular weight forms more rigid nanonetworks.

Acknowledgement

This work is supported by National Science Foundation under Grant DMR-0346435.

References

[1] Krishnamoorti R, Vaia RA. Polymer nanocomposites – synthesis, characterization and modeling. In: ACS symposium series, vol. 804. Washington DC: ACS; 2001.
[2] Whitesides GM, Mathias TP, Seto CT. Science 1991;254:1312.
[3] Nalwa HS. Handbook of organic–inorganic hybrid materials and nanocomposites. In: Nanocomposites, vol. 2. Stevenson Ranch, California: American Scientific Publishers; 2003.
[4] Pielichowski K, Njuguna J, Janowski B, Pielichowski J. Adv Polym Sci 2006;201:225.
[5] Lucke S, Stoppek-Langner K. Appl Surf Sci 1999;145:713.
[6] Schwab JJ, Lichtenhan JD. Appl Organomet Chem 1998;12:707.
[7] Li GZ, Wang LC, Ni HL, Pittman CU. J Inorg Organomet Polym 2001;11:123.
[8] Lichtenhan JD, Noel CJ, Bolf AG, Ruth PN. Mater Res Soc Symp Proc 1996;435:3.
[9] Lichtenhan JD. Comments Inorg Chem 1995;17:115.
[10] Fu BX, Hsiao BS, Pagola S, Stephens P, White H, Rafailovich M, et al. Polymer 2001;42:599.
[11] Haddad TS, Lichtenhan JD. Macromolecules 1996;29:7302.
[12] Mather PT, Jeon HG, Romo-Uribe A, Haddad TS, Lichtenhan JD. Macromolecules 1998;32:1194.
[13] Zheng L, Farris RJ, Coughlin EB. Macromolecules 2001;34:8034.
[14] Xu HY, Kuo SW, Lee JS, Chang FC. Macromolecules 2002;35:8788.
[15] Xu HY, Kuo SW, Chang CF. Polym Bull (Berlin) 2002;48:469.
[16] Schwab JJ, Haddad TS, Lichtenhan JD, Mather PT, Chaffee KP. Annual Technical Conference – Society of Plastics Engineers 1997;611:1817.
[17] Kopesky ET, Haddad TS, Cohen RE, Mckinley GH. Macromolecules 2004;37:8992.
[18] Fu BX, Gelfer MY, Hsiao BS, Phillips S, Viers B, Blanski R, et al. Polymer 2003;44:1499.
[19] Joshi M, Butola BS, Simon G, Kukaleva N. Macromolecules 2006;39:1839.
[20] Capaldi FM, Rutledge GC, Boyce MC. Macromolecules 2005;38:6700.
[21] Romo-Uribe A, Mather PT, Haddad TS, Lichtenhan JD. J Polym Sci Part B Polym Phys 1998;36:1857.
[22] Huang C, Kuo S, Lin F, Huang W, Wang C, Chen W, et al. Macromolecules 2006;39:300.
[23] Liu H, Zheng S, Nie K. Macromolecules 2005;38:5088.
[24] Drazkowski DB, Lee A, Haddad TS, Cookson DJ. Macromolecules 2006;39:1854.
[25] Bizet S, Galy J, Gerard J. Macromolecules 2006;39:2574.
[26] Tsuchida A, Bolln C, Sernetz FG, Frey H, Mulhaupt R. Macromolecules 1997;30:2818.
[27] Turri S, Levi M. Macromolecules 2005;38:5569.
[28] Zheng L, Hong S, Cardoen G, Burgaz E, Gido SP, Coughlin EB. Macromolecules 2004;37:8606.
[29] Liang K, Toghiani H, Li G, Pittman CU. J Polym Sci Part A Polym Chem 2005;43:3887.
[30] Li G, Cho H, Wang LC, Toghiani H, Pittman CU. J Appl Polym Sci Part A Polym Chem 2005;43:355.
[31] Li G, Thompson T, Daulton TL, Pittman CU. Polymer 2002;43:4167.
[32] Cho H, Liang K, Chatterjee S, Pittman CU. J Inorg Organomet Polym Mater 2005;15:541.
[33] Li G, Wang LC, Toghiani H, Daulton TL, Koyama K, Pittman CU. Macromolecules 2001;34:8686.
[34] Liang K, Li G, Toghiani H, Koo JH, Pittman CU. Chem Mater 2006;18:301.
[35] Patel RR, Mohanraj R, Pittman CU. J Polym Sci Part B Polym Phys 2006;44:234.
[36] Zhang Y, Lee S, Yoonessi M, Liang K, Pittman CU. Polymer 2006;47:2984.
[37] Chen W, Wang Y, Kuo S, Huang C, Tung P, Chang F. Polymer 2004;45:6897.
[38] Choi J, Kim SG, Laine RM. Macromolecules 2004;37:99.
[39] Choi J, Harcup J, Yee AF, Zhu Q, Laine RM. J Am Chem Soc 2001;123:11420.
[40] Choi J, Yee AF, Laine RM. Macromolecules 2004;37:3267.
[41] Choi J, Tamaki R, Kim SG, Laine RM. Chem Mater 2003;15:3365.
[42] Kim GM, Qin H, Fang X, Sun FC, Mather PT. J Polym Sci Part B Polym Phys 2003;41:3299.
[43] Tamaki R, Choi J, Laine RM. Chem Mater 2003;15:793.
[44] Ni Y, Zheng S, Nie K. Polymer 2004;45:5557.
[45] Bian Y, Pejanovic S, Kenny J, Mijovic J. Macromolecules 2007;40:6239.
[46] Strachota A, Kroutilova I, Kovarova J, Matejka L. Macromolecules 2004;37:9457.
[47] Matejka L, Strachota A, Plestil J, Whelan P, Steinhart M, Slouf M. Macromolecules 2004;37:9449.
[48] Romirez C, Abad MJ, Barral L, Cano J, Diez FJ, Lopez J, et al. J Therm Anal Calorim 2003;72:421.
[49] Abad MJ, Barral L, Fasce DP, Williams RJJ. Macromolecules 2003;36:3128.
[50] Yoon KH, Polk MB, Park JH, Min BG, Schiraldi DA. Polym Int 2005;54:47.
[51] Yei D, Kuo S, Su Y, Chang F. Polymer 2004;45:2633.
[52] Xu H, Yang B, Wang J, Guang S, Li C. Macromolecules 2005;38:10455.
[53] Lichtenhan JD, Otonari YA, Carr MJ. Macromolecules 1995;28:8435.
[54] Chen Y, Kang E. Mater Lett 2004;2004:3716.
[55] Mather PT, Jeon HG, Romo-Uribe A, Haddad TS, Lichtenhan JD. Macromolecules 1999;32:1194.
[56] Stockmayer WH, Baur ME. J Am Chem Soc 1964;86:3485.
[57] Adachi K, Kotaka T. Prog Polym Sci 1993;18:585.
[58] Watanabe H. Prog Polym Sci 1999;24:1253.
[59] Watanabe H. Macromol Rapid Commun 2001;22:127.
[60] Adachi K. Dielectric spectroscopy of polymeric materials. Washington DC: American Chemical Society; 1997. p 261–82 [chapter 9].

[61] Mijovic J, Han Y, Sun M, Pejanovic S. Macromolecules 2003;36:4589.
[62] Mijovic J, Bian Y, Gross RA, Chen B. Macromolecules 2005;38:10812.
[63] Williams G. Theory of dielectric properties, in dielectric spectroscopy of polymeric materials. Washington DC: American Chemical Society; 1997.
[64] Williams G. Dielectric relaxation spectroscopy of amorphous polymer systems: the modern approaches [chapter 1]. In: Keynote lectures in selected topics of polymer science. Madrid: CSIC; 1997. p. 1–40.
[65] Kremer F. Broadband dielectric spectroscopy. Berlin: Springer-Verlag; 2002.
[66] Mijovic J, Sun M, Han Y. Macromolecules 2002;35:6417.
[67] Havriliak Jr S, Negami S. Polymer 1967;8:161.
[68] Kremer F, Schonhals A. Broadband dielectric spectroscopy. Berlin: Springer-Verlag; 2002.
[69] Cole RH, Cole KS. J Chem Phys 1942;10:98.
[70] Bian Y, Mijovic J. Macromolecules 2008;41:7122.